# Optical properties of liquid nickel and iron

Shankar Krishnan, Koji J. Yugawa, and Paul C. Nordine
*Containerless Research, Inc., Evanston, Illinois 60201*
(Received 4 March 1996; revised manuscript received 4 December 1996)

The optical properties of pure liquid nickel and iron were investigated in the energy range 1.2–3.5 eV. Nickel and iron specimens were electromagnetically levitated, melted, and purified of residual oxide contaminants by heating to elevated temperatures and/or reacting the liquids with pure hydrogen. An automated dual-detector rotating analyzer ellipsometer with a pulsed-dye-laser light source was employed to measure the optical properties. Measurements were obtained over the full energy range at 1764 K for nickel and at 1890 K for iron. Liquid nickel exhibited a broad minimum in the optical conductivity at about 2.2 eV photon energy, similar to the minimum that the solid exhibits at about 3 eV. The optical conductivity of liquid iron increased smoothly from the UV to the IR except in the vicinity of 2.25 eV where a 10% decrease was observed. This behavior is quite different from the solid, which shows a broad peak in the optical conductivity at about 2.4 eV and decreasing conductivity values towards the UV and IR. A broad minimum was also observed in the real part of the dielectric constant for liquid iron, at about 2.0 eV, where a maximum occurs for the room-temperature ferromagnetic solid. The optical properties and spectral emissivities of liquid nickel and iron are discussed with respect to available literature data for both the solid and liquid. [S0163-1829(97)03613-8]

## I. INTRODUCTION

There are few published results on the optical properties of liquid transition metals at high temperatures. These properties are needed to advance theories of condensed matter physics, to estimate radiative energy balances, and for temperature measurements using radiometric devices during thermophysical property measurements. In this study, we report measurements of the optical properties of liquid nickel and iron at elevated temperatures over a photon energy range 1.2–3.5 eV, i.e., over a wavelength range of about 990–360 nm.

The optical properties of solid nickel have been investigated by several researchers including Ehrenreich *et al.*,[1] Lynch *et al.*,[2] and Vehse and Arakawa,[3] and there is excellent agreement in the results obtained over a wide energy range. A summary of the optical properties of solid nickel is given in Ref. 4. The optical conductivity increases in the UV and peaks at approximately 4.5 eV photon energy. Liquid nickel was investigated in the energy range 2.25–5 eV by Miller,[5] who found the optical conductivity to be 5000 $(\Omega\ \mathrm{cm})^{-1}$ and nearly independent of energy.

The optical properties of solid iron have been investigated by Weaver *et al.*,[6] Moravec *et al.*,[7] Yolken and Kruger,[8] and others. The results confirm the existence of a sharp peak in the optical conductivity around 2.4 eV for solid iron, which was attributed by Weaver *et al.*[6] to contributions from multiple bands. The few data that have been obtained for liquid iron[5] show little structure in the optical conductivity in the energy range 2.25–5 eV with values approximately equal to 5000 $(\Omega\ \mathrm{cm})^{-1}$.

These previous measurements on liquid iron and nickel[5] were conducted on specimens contained in alumina crucibles. If the starting iron specimens contained approximately 1 mol % dissolved oxygen atoms, an oxygen-rich liquid would precipitate from the liquid iron pool. The existence of two liquids in the Fe-O phase diagram near the melting point of pure iron is well known.[9] On the other hand, liquid nickel is less sensitive to oxygen impurities because (i) more than 2 mol % dissolved oxygen atoms is required[9] before the solid NiO phase will precipitate from the liquid and (ii) the oxygen decomposition pressure is much greater for solid NiO than for the oxygen-rich liquid in the Fe-O system. As a result of the higher oxygen decomposition pressure for nickel, considerable purification occurs for levitated liquid nickel. Purification of liquid iron can be achieved by a reaction with pure hydrogen to reduce the oxygen-rich phase.

A unique feature of the present work is the use of containerless methods for the investigation of liquid metal optical properties. The liquid specimens were levitated and heated in an electromagnetic field to eliminate container interactions and contamination. A pulsed dye laser was used as a light source with high spectral resolution, and ellipsometric measurements were obtained on liquid nickel and iron over the 1.2–3.5-eV photon energy range. The apparatus, methods, and error analyses are given in previous publications on the optical properties of liquid aluminum,[10,11] zirconium,[12] and nickel-based alloys.[13]

## II. EXPERIMENTAL DETAILS

### A. Levitation system

The experimental methods used in the present work were essentially the same as in previous investigations on liquid aluminum,[10] zirconium,[12] and nickel-based alloys.[13] Electromagnetic (EM) levitation and heating were used to suspend and melt the specimens inside a high-vacuum chamber using a 5-kW radio-frequency generator that operated at ~450 kHz. Specimen masses were 0.30–0.40 g and 4–5-mm-diam liquid droplets formed during the experiments.

Laser ellipsometric measurements were conducted on the levitated liquid drops to measure the optical properties over the 1.2–3.5 photon energy range of a dye-laser source. The incoming laser beam illuminated approximately 50% of the

 

curved specimen surface where it was reflected into a large cone. The analyzer collected a small fraction ($\pm 1.8°$ cone angle) of the reflected light at the fixed, prealigned 67.5° angle of incidence.

Apparent (radiance) temperatures of the specimens were measured using two calibrated optical pyrometers (Pyro Photo II, Pyrometer Instrument Company, Northvale, NJ) whose operating wavelengths were approximately 650 nm. Concurrently, infrared radiance measurements were obtained with a pyrometer developed by Heimann Optoelectronics GMBH (model KT-19.99). This pyrometer had a bandwidth of 1–2.5 $\mu$m with an effective wavelength of about 2.0 $\mu$m. A $CaF_2$ window was used on the levitation chamber for measurements with the infrared pyrometer, and sapphire or BK7 windows were used for the two 650-nm pyrometers. Window transmission corrections for the radiance temperature were independently determined. The spectral emissivities of the liquid materials were derived from the ellipsometric measurements at the pyrometer wavelength (0.65 $\mu$m). The true specimen temperature was calculated using the measured 0.65-$\mu$m radiance temperatures, the window corrections, and the measured spectral emissivities. Approximate values of the normal spectral emissivities in the wave band of the infrared pyrometer were derived from the true surface temperature and the measured infrared radiance temperatures.

### B. Ellipsometry

A pulsed-dye-laser ellipsometer system was used to obtain the optical property measurements. A Molectron DL-II dye laser provided laser radiation in the wavelength range 360–990 nm (photon energy range 3.44–1.25 eV). The laser pulse width was 7 ns, and it was operated at a repetition rate of 20 Hz. The source optics included a two-axis beam steering device, followed by a 0.3-cm aperture and two Glan-Thomson linear polarizers. The second polarizer was fixed at $+45°$ with respect to the plane of incidence. The first polarizer could be rotated to adjust the light intensity to 1 mJ or less in a 0.3-cm-diam beam.

The design of the analyzer optics was based on the original work of Beattie[14] and its modification developed by Krishnan and Nordine.[10] A beam-splitting Glan-Thomson prism provided orthogonal components of the polarization for simultaneous detection. The beam deviation between the two orthogonal components was 45°, independent of wavelength. Measurements of the light intensities could simultaneously be recorded for individual azimuth pairs of {0°, 90°} and {45°, −45°} or {135°, 45°} by rotating the analyzer assembly to three fixed orientations. The use of interference filters and specialized detector electronics to minimize the effects of incandescent specimen radiation is described in earlier publications.[10,12]

The measured values of $\psi$ and $\Delta$ were used to calculate the real and imaginary parts of the indices of refraction, $N = n - ik$, from[16]

$$N = n - ik = n_0 \tan\phi \left[ 1 - \frac{4\rho}{(1+\rho)} \sin^2\phi \right]^{1/2}, \tag{1}$$

where $\rho$ is the complex reflectance defined by

$$\rho = \tan\psi e^{i\Delta}. \tag{2}$$

Values of the normal incidence reflectivity were calculated from the expression

$$R_\lambda = \frac{(n-n_0)^2 + k^2}{(n+n_0)^2 + k^2}, \tag{3}$$

where $n_0$ is the refractive index of the ambient (transparent) medium. Quantities of interest given in this paper include the real part of the complex dielectric function, $\epsilon_1 = n^2 - k^2$, the optical conductivity $\sigma = 4\pi\epsilon_0 nk\nu$, and the spectral emissivity (or absorptivity) $\epsilon_\lambda = 1 - R_\lambda$, which are all quantities derived from the ellipsometric measurements.

The method used to calibrate the ellipsometer has been described by Hunderi and Ryberg[15] and is described in detail in earlier publications.[10,12] Calibration of the ellipsometer was done prior to the start of this work and confirmed at the conclusion of the work.

### C. Specimens and purification

Rods of iron and nickel were obtained from ESPI Inc., Ashland, OR. The nickel was stated to be 99.9995% pure, and the iron was stated to be 99.95% pure. Specimens of approximately 300 mg were cut from the rods and cleaned in alcohol and acetone prior to EM levitation.

All of the experiments were conducted under pure helium and argon atmospheres. The inert atmosphere resulted in a convective heat loss that allowed the specimen temperatures to be maintained at sufficiently small values at the EM power necessary for levitation. The inert gas atmosphere also minimized vaporation of the metals during the extended duration of the experiments.

Once the specimens were levitated, melting usually occurred within about 10 s for both nickel and iron. The specimens were initially heated to approximately 200–300 K above their melting points of 1729 K for nickel and 1808 K for iron to vaporize any contaminants. In the case of nickel, the oxide decomposition pressure was sufficient to provide rapid removal of any oxide impurities that were present. Once this occurred, the specimen surfaces remained extremely clean throughout the optical measurements. For iron, the oxide decomposition pressure was not sufficient, and residual oxide was removed by reaction with hydrogen gas prior to optical measurements. This was achieved by filling the levitation chamber with a mixture of the inert gas (argon and helium) and pure hydrogen. The hydrogen concentration was typically 10%. It is known that iron has a high solubility for hydrogen, and dissolved hydrogen could influence the optical properties. Therefore two sets of optical property measurements were obtained on liquid iron, one with hydrogen and one in pure inert gas. The results were essentially identical, implying that either (i) there was little or no oxide present in the liquid at the beginning or (ii) any dissolved hydrogen did not significantly affect the optical properties.

Temperature fluctuations on the order of $\pm 2$ K occurred between measurements at different azimuths of the analyzer. Specimen temperatures were cycled between high and low temperatures over the duration of the measurements to eliminate any systematic differences, none of which were observed. Measurements of the optical properties over the en-

tire wavelength range were conducted at a mean temperature of $1764\pm10$ K for liquid nickel and at $1890\pm10$ K for liquid iron.

After optical property measurements were completed on a given specimen, the specimens were allowed to undercool by flowing helium gas into the system and reducing the EM power. The undercooling was typically greater than 250 K (for both nickel and iron). Hydrogen reduction of residual iron oxides was required to achieve this result with iron. The undercooling results established that the optical property measurements were made on clean liquid metal surfaces, since the presence of contaminants (e.g., oxide impurities) will generally cause heterogeneous nucleation of the solid phase and prevent significant undercooling. The data for nickel and iron were obtained on multiple specimens. Optical property results were obtained over a limited wavelength range for each specimen with some overlapping wavelength regions.

## III. RESULTS

The absolute accuracy of the measurements of the optical conductivity and the dielectric functions was influenced by three factors. First, a small error resulted because the properties were calculated using the mean angle of incidence, while a cone of reflected light was analyzed for its polarization. The incident laser beam divergence, less than 1 mrad, was negligible. Second, the ellipsometer calibration function was estimated to have errors as large as $\pm1\%$, which would vary with wavelength. The errors from these first two sources were similar to the analyzed errors reported previously[10,12] in measurements on liquid Al and Zr.

The third source of errors was in the six detector voltage measurements used to derive the optical property results corresponding to each wavelength. The absolute precision of these voltage measurements was constant, while the magnitude of each voltage measurement varied with the optical properties and adjustments to the incident light source. The propagation of voltage errors in the optical property calculations was analyzed for each result. In some cases, large optical property errors occurred as a result of small voltages being measured on one or more of the detectors. These results were rejected. The remaining data are presented in the following plots, with error bars that represent the analyzed precision of measurements given at three different wavelengths or photon energies.

### A. Optical properties

Figure 1 shows the measured values of the optical conductivity $\sigma$ for liquid nickel at $T=1764\pm10$ K as a function of photon energy (solid symbols). Data from the literature for solid nickel at room temperature are shown by the dashed line, and results for the liquid reported by Miller[5] are given by the open circles. The data for the liquid obtained in this work resemble the data for the solid, with a minimum in the conductivity at about 2.2 eV. However, the liquid appears to show considerable broadening of the trough. The data of Miller [5] at energies greater than 2 eV are in good agreement with the present results. The agreement is also good for the $\epsilon_1$ vs energy data given in Fig. 2.

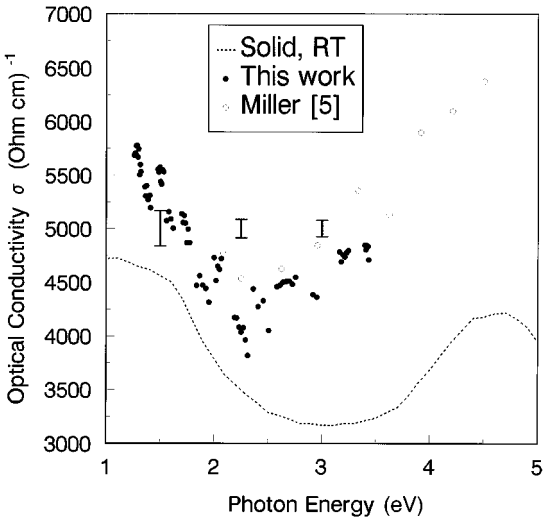


FIG. 1. Optical conductivity $\sigma$ for liquid nickel at $1764\pm10$ K as a function of photon energy. The data from the present work are given by the solid circles, the data for liquid nickel at the melting point from Miller (Ref. 5) are given by the open circles, and the data for the ferromagnetic solid at room temperature (Ref. 4) are given by the dashed line. The error bars illustrate the analyzed uncertainty in the results at three photon energies.

The data for liquid iron are given in Figs. 3 and 4. Figure 3 is a plot of the optical conductivity for liquid iron at a temperature of $1890\pm10$ K as a function of the incident photon energy. The results obtained in this work are given by the solid circles. The data from Miller[5] are the open circles. The dashed line is the data for the ferromagnetic solid at room temperature obtained from Weaver *et al.*[6] The $\epsilon_1$ data are plotted in Fig. 4, together with the literature data. The present results agree well with the data of Miller[5] for both

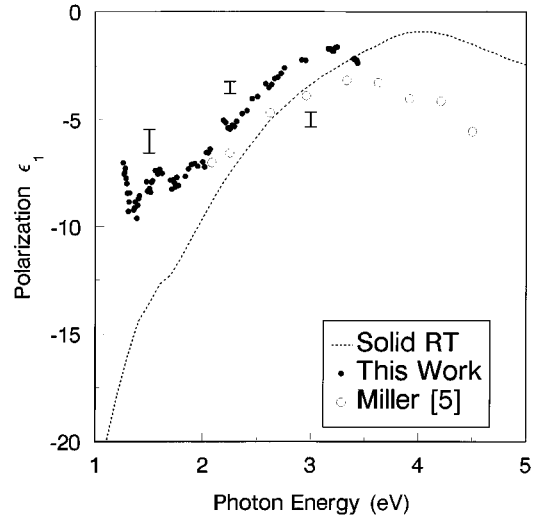


FIG. 2. Real part of the dielectric constant $\epsilon_1$ for liquid nickel at $1764\pm10$ K as a function of photon energy. The data from the present work are given by the solid circles, the data for liquid nickel at the melting point from Miller (Ref. 5) are given by the open circles, and the data for the ferromagnetic solid at room temperature (Ref. 4) are given by the dashed line. The error bars illustrate the analyzed uncertainty in the results at three photon energies.

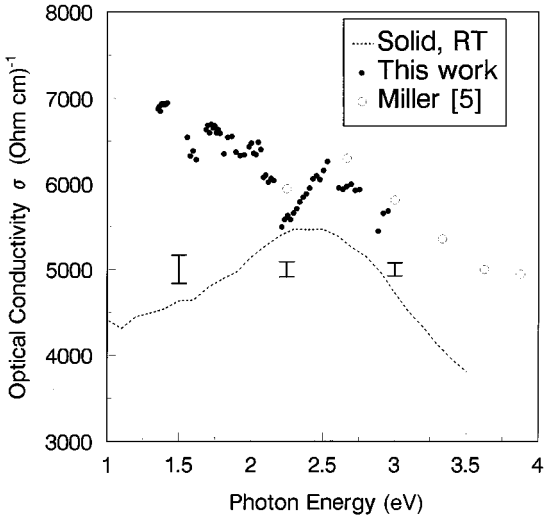


FIG. 3. Optical conductivity $\sigma$ for liquid iron at $1890\pm10$ K as a function of photon energy. The data from the present work are given by the solid circles, the data for liquid iron at the melting point from Miller (Ref. 5) are given by the open circles, and the data for the ferromagnetic solid at room temperature (Ref. 6) are given by the dashed line. The error bars illustrate the analyzed uncertainty in the results at three photon energies.

the optical conductivity and polarization. The minimum in the conductivity near 2.25 eV shown by the present data is supported by the two points obtained by Miller in this photon energy range. The rapid decrease and then increase in the conductivity between 2.1 and 2.5 eV occurs where $\epsilon_1$ shows a minimum. The variations in $\sigma$ in this energy range are well outside the analyzed errors in $\sigma$ values as shown by the error bar in Fig. 3. The minimum in $\sigma$ was also observed in preliminary experiments.

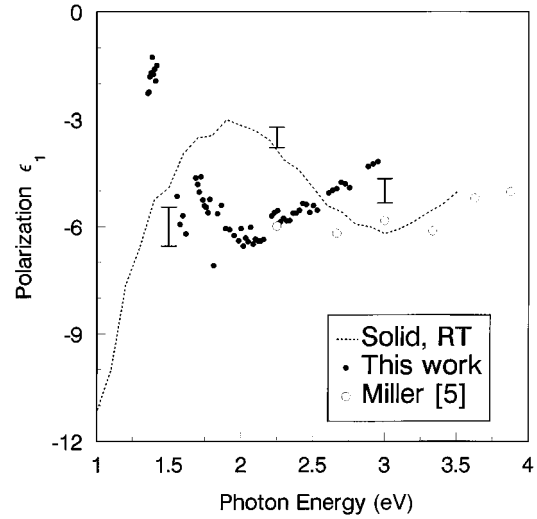


FIG. 4. Real part of the dielectric constant $\epsilon_1$ for liquid iron at $1890\pm10$ K as a function of photon energy. The data from the present work are given by the solid circles, the data for liquid iron at the melting point from Miller (Ref. 5) are given by the open circles, and the data for the ferromagnetic solid at room temperature (Ref. 6) are given by the dashed line. The error bars illustrate the analyzed uncertainty in the results at three photon energies.

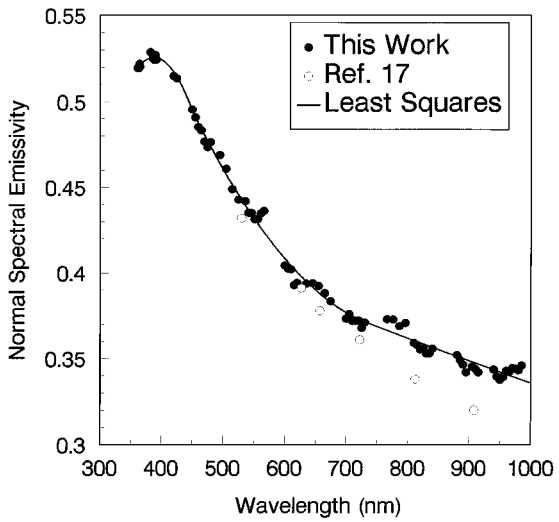


FIG. 5. Normal spectral emissivity (or absorptivity) as a function of wavelength for liquid nickel. The data obtained in the present work are shown by solid circles and correspond to a mean temperature of $1764\pm10$ K. The solid line is a multifunctional least-squares fit to the data. The open circles are unpublished data (Ref. 17).

### B. Emissivity

The normal spectral emissivity (or absorptivity) was obtained from measurements of the optical constants [see Eq. (3)]. Figure 5 shows the normal spectral emissivity of liquid nickel at $1764\pm10$ K as a function of wavelength in the 370–1000-nm range of our measurements. The solid line is a least-squares fit to the data that included the value of the emissivity obtained indirectly from infrared pyrometry corresponding to a wavelength of 2.0 $\mu$m. Three separate functions were used to fit these data for Ni in three separate wavelength ranges. Also shown on the plot are six open circles corresponding to normal spectral emissivity values for nickel at the melting point measured by optical pyrometric methods.[17] Except at 908 nm, the present data and the pyrometric results agree within the combined uncertainties of the two sets of results.

The spectral emissivity data for liquid iron at $1890\pm10$ K are given as a function of wavelength in Fig. 6. Unpublished results of Cezairliyan and McClure[17] are shown by open circles. The present data and the unpublished pyrometric results[17] agree within the combined errors, except at wavelengths of 812 and 908 nm. Two separate functions were used to fit the spectral emissivity data over the range shown.

Values of the spectral emissivity were also obtained at $\lambda\approx2.0$ $\mu$m from radiance temperature measurements using the infrared pyrometer. Spectral emissivity values for $\lambda=2.0$ $\mu$m for liquid nickel were calculated to be $0.231\pm0.01$ and for liquid iron as $0.270\pm0.01$.

## IV. DISCUSSION

### A. Optical properties

The present results show the optical properties of liquid and solid nickel have much similarity. In contrast, the optical properties of solid and liquid iron are quite different. In nickel and iron the *d* bands overlap the Fermi level, and in

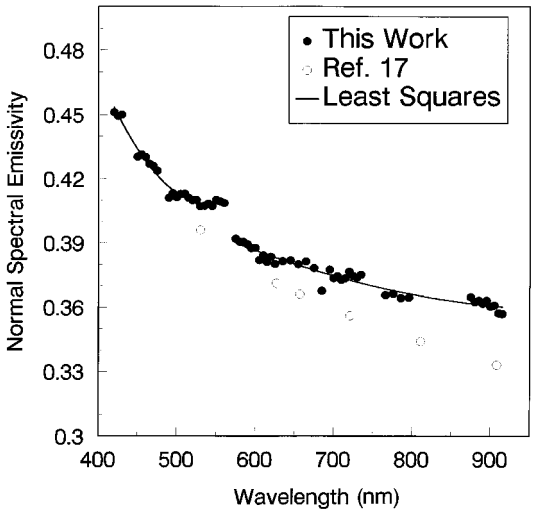


FIG. 6. Normal spectral emissivity (or absorptivity) as a function of wavelength for liquid iron. The data obtained in the present work are shown by solid circles and correspond to a mean temperature of 1890±10 K. The solid line is a multifunctional least-squares fit to the data. The open circles are unpublished data (Ref. 17).

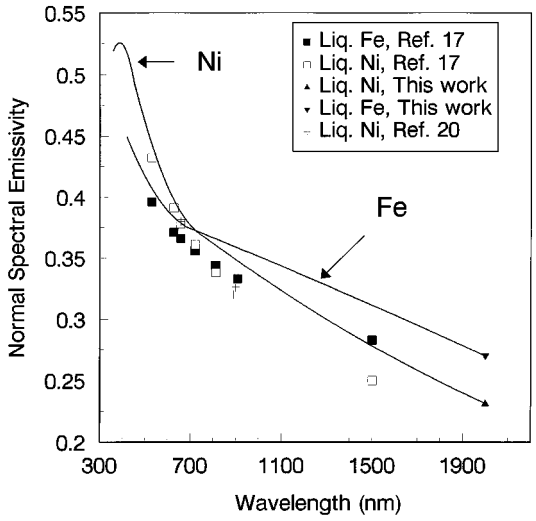


FIG. 7. Normal spectral emissivity functions for liquid nickel and iron together with the value in the infrared at 2.0 $\mu$m. Data from the literature (Refs. 17 and 20) are included in the plot. The solid lines are the multifunctional fits to the experimentally measured results obtained in this work.

the solid state below the Curie point the *d* bands are split as a result of the exchange interaction giving rise to ferromagnetism. Therefore there can be no direct comparison of the results for the liquid with those for the room-temperature solid. However, Shiga and Pells[18] have observed that the absorption spectrum for nickel does not change much through the Curie temperature.

For nickel an absorption minimum is observed for the liquid at about 2.2 eV similar to that for the solid at 3 eV. This shift may be explained by a widening of the Fermi distribution function at the elevated temperatures, assuming that the electronic structure is similar for the solid and liquid. Alternatively, the shift may be attributed to a greatly increased absorption in the UV relative to that in the IR region. Liquid and solid nickel exhibit similar conductivity values in the infrared, but the conductivity values over the full energy range are larger for the liquid than for the solid. In conclusion, the optical properties of liquid nickel have much similarity with the solid over the photon energy range investigated and the optical conductivity increases more in the UV upon melting than in the IR.

For liquid iron the optical conductivity data are in good agreement with the data of Miller[5] in the overlapping wavelength range. Our measurements at longer wavelengths show that $\epsilon_1$ has a minimum at about 2.0 eV. The minimum in $\sigma$ for liquid iron at 2.25 eV is consistent with the two measurements reported by Miller[5] in the same energy range. Unlike nickel, there is little correspondence between the optical properties of solid and liquid iron. This difference might result from the fact that ferromagnetic contributions to the optical properties of nickel lie outside the wavelength range investigated in this work, but for iron are substantial in the visible and near-IR spectral range. It would be interesting to measure the optical properties of iron above the Curie temperature where the present results on nickel and our previously reported results on aluminum and zirconium suggest that the optical properties of solid iron may be quite similar to those of liquid iron.

Miller[5] remarked that the absorption in liquid iron, cobalt, and nickel was almost independent of photon energy and approximately equal to 5000 $(\Omega\ \text{cm})^{-1}$. Miller's conclusion was based on optical property data that did not extend below 2 eV photon energy. Our data reveal that there is 20% or greater variability in the absorption curves for liquid iron and nickel in the 1–3.5-eV photon energy range. Our data also show that the magnitude of the absorption for liquid iron is about 20% larger than that for liquid nickel and confirm that the optical conductivity for the liquids is greater than for the corresponding solid phases.

### B. Emissivity

The emissivity data for liquid nickel and iron in Figs. 5 and 6 show a common behavior exhibited by many metals, namely, a monotonic decrease in the emissivity with wavelength and a slowly decreasing slope.[19] Approximate values of emissivity at $\lambda=2.0$ $\mu$m were also obtained in this work. Figure 7 plots the emissivity data for both liquid nickel and iron with the infrared results included as solid triangles. The solid lines in Fig. 7 represent the multifunction polynomial fits to the data that include the measured values at $\lambda=2.0$ $\mu$m. Literature data for liquid nickel and iron obtained from two sources[17,20] are also shown in the plot and identified on the legend.

The present data agree well with the literature results in the visible region (i.e., $<$800 nm), but the differences increase in the infrared such that they exceed the combined errors of the two sets of results at longer wavelengths. The literature results[17,20] depicted in Fig. 7 were obtained at the melting point during rapid pulse heating of iron and nickel specimens.

One reason for the difference may be due to the presence of a thin oxide layer on the pulse-heated specimens. If any residual oxide was present on the specimen surfaces, there may not have been sufficient time for these oxides to dis-

solve or vaporize. If a thin oxide layer was present during the pulse-heating experiments on nickel and iron, its influence would depend on the layer thickness, the wavelength, and the optical properties of the oxide and substrate liquid. One would expect greater scatter between experiments in the presence of the oxide.

The results show a decrease of emissivity with wavelength that is typical of metals. Metals also typically show only small variations of emissivity with temperature in the visible region, where the present and radiometric results agree, and a significant increase of emissivity with temperature in the infrared. Since the present results were obtained at temperatures above the melting point (40 K for nickel and 80 K for iron), the effect of temperature probably contributes to the differences with the radiometric results.

The data in Fig. 7 confirm the strong wavelength dependence typical of transition metals. For Ni, the spectral emissivity decreases approximately 0.15 per 1 $\mu$m and for iron the decrease is approximately 0.12 per 1 $\mu$m in the 0.3–2.0-$\mu$m wavelength range. The data may be directly used to compute other radiative properties such as the spectral hemispherical emissivity. The total hemispherical emissivity could be obtained by extending the optical measurements to longer wavelengths where a majority of the radiant energy is emitted by specimens at the temperatures of interest.

## V. CONCLUSIONS

The optical properties of levitated liquid nickel and iron were studied by pulsed-dye-laser spectroscopic ellipsometry. The results show some structure in the optical conductivity and polarization spectra in the 1.25–3.5-eV photon energy range. For liquid nickel, an approximately 0.8-eV IR shift in the absorption minima was observed relative to the room-temperature solid. Liquid iron has an optical property spectrum quite different from the solid. There is good agreement in the data for liquid nickel and iron between the present work and the previous results of Miller[5] at photon energies greater than 2 eV. The present results for nickel show a minimum in the optical conductivity spectrum near 2.2 eV that is supported, but not clearly shown, by the data of Miller.[5] This observation was possible due to the high spectral resolution used in the present work and the large number of measurements obtained for the liquid. There is also good agreement in the normal spectral emissivity values in the visible region of the spectrum with reported literature results, but the agreement decreases at wavelengths greater than 800 nm.

This work adds to our previous work on liquid aluminum,[10,11] zirconium,[12] and nickel-based alloys,[13] where considerable structure in the electronic properties was observed. The observations of this structure in iron and nickel and the similarity of solid and liquid properties for nickel support the idea that liquid metals have solidlike optical properties.

## ACKNOWLEDGMENTS

This work was supported by Grant No. NASW-4687 from the National Aeronautics and Space Administration, Microgravity Sciences and Applications Division.

[1] H. Ehrenreich, H. R. Philipp, and D. J. Olechna, Phys. Rev. **131**, 2469 (1963).
[2] D. W. Lynch, R. Rosei, and J. H. Weaver, Solid State Commun. **9**, 2195 (1971).
[3] R. E. Vehse and E. T. Arakawa, Phys. Rev. **180**, 695 (1969).
[4] D. W. Lynch and W. R. Hunter, in *Handbook of Optical Constants of Solids*, edited by Edward D. Palik (Academic, New York, 1985).
[5] J. C. Miller, Philos. Mag. **20**, 1115 (1969).
[6] J. H. Weaver, E. Colavita, D. W. Lynch, and R. Rosei, Phys. Rev. B **19**, 3850 (1979).
[7] T. J. Moravec, J. C. Rife, and R. N. Dexter, Phys. Rev. B **13**, 3297 (1976).
[8] H. T. Yolken and J. Kruger, J. Opt. Soc. Am. **55**, 842 (1965).
[9] *Binary Alloy Phase Diagrams*, edited by J. L. Murray, L. H. Bennett, and H. Baker (American Society for Metals, Metals Park, OH, 1986).
[10] S. Krishnan and P. C. Nordine, Phys. Rev. B **47**, 11 780 (1993).
[11] S. Krishnan and P. C. Nordine, Phys. Rev. B **48**, 4130 (1993).
[12] S. Krishnan and P. C. Nordine, Phys. Rev. B **49**, 3161 (1993).
[13] S. Krishnan and P. C. Nordine, J. Appl. Phys. **80**, 1735 (1996).
[14] J. R. Beattie, Philos. Mag. **46**, 235 (1955).
[15] O. Hunderi and R. Ryberg, Surf. Sci. **56**, 182 (1976).
[16] R. M. A. Azzam and N. M. Bashara, *Ellipsometry and Polarized Light* (North-Holland, New York, 1987).
[17] A. Cezirliyan and J. L. McClure (private communication).
[18] H. Shiga and G. P. Pells, J. Phys. C **2**, 1847 (1969).
[19] S. Roberts, Phys. Rev. **114**, 104 (1959).
[20] F. Righini (unpublished).